Investigation of the Response of Electrical Insulator Posts Using Real-Time Hybrid Simulation on a Smart Shaking Table

M.S. Günay, K.M. Mosalam
University of California, Berkeley

SUMMARY
A real-time hybrid simulation (RTHS) framework is developed for efficient dynamic testing of electrical insulator posts on a smart shaking table. The framework consists of the insulator post, a 4 ft×4 ft shaking table, a state-of-the-art controller and a digital signal processor. Explicit Newmark method is adopted for the numerical integration of the governing equation of motion of the hybrid structure, which consists of an insulator post (experimental substructure) and a spring-mass-dashpot system representing the support structure of the insulator (analytical substructure). Two of the unique features of the developed RTHS framework are the application of a simple feed-forward error compensation scheme and the ability to use integration time steps as small as 1 millisecond. After validation of the developed RTHS framework with the results of a conventional shaking table test, a parametric study is conducted to investigate the effect of support structure stiffness and damping on the insulator response.

Keywords: Electrical insulator post, real time hybrid simulation, smart shaking table, support structure

1. INTRODUCTION

Disconnect switches constitute a crucial component of power transmission and distribution systems. They are used to control the flow of electricity between all types of substation equipment. Electrical insulator posts and a metallic tube that resides between the top of the insulator posts comprise a typical disconnect switch. In the field, disconnect switches are generally mounted on support structures, which are typically steel frames or columns with well-defined geometry (Fig. 1.1). IEEE693-2005 (IEEE, 2006) requires seismic qualification verification of the disconnect switches by conducting shaking table tests. According to this requirement, a disconnect switch and its accompanying support structure is constructed, mounted to a shaking table and tested as shown in Fig. 1.2.

Structural and corresponding dynamic properties of the support structures have considerable effect on the response of the disconnect switches. Therefore, there may be a need for an iterative shaking table test scheme based on the modification of the structural configuration of the support structure until the acceptable performance of the tested disconnect switch is achieved. However, conducting a series of this type of conventional shaking table tests is time-consuming and economically unfeasible. In that regard, hybrid simulation (HS), which allows representation of support structures with well-defined material and geometrical properties as analytical substructures, comes forward as a cost effective and efficient testing method alternative to the conventional shaking table testing of the disconnect switches. The rate-dependent nature of some types of insulators, e.g. polymer composite insulators, mandates the use of real-time hybrid simulation (RTHS). The distributed mass of the insulators limits the practical use of actuators at concentrated locations along the height of the insulator and necessitates RTHS to be conducted on smart shaking table configurations. Therefore, a RTHS framework is developed in this paper for testing insulator posts of the disconnect switches to satisfy the above mentioned objectives.

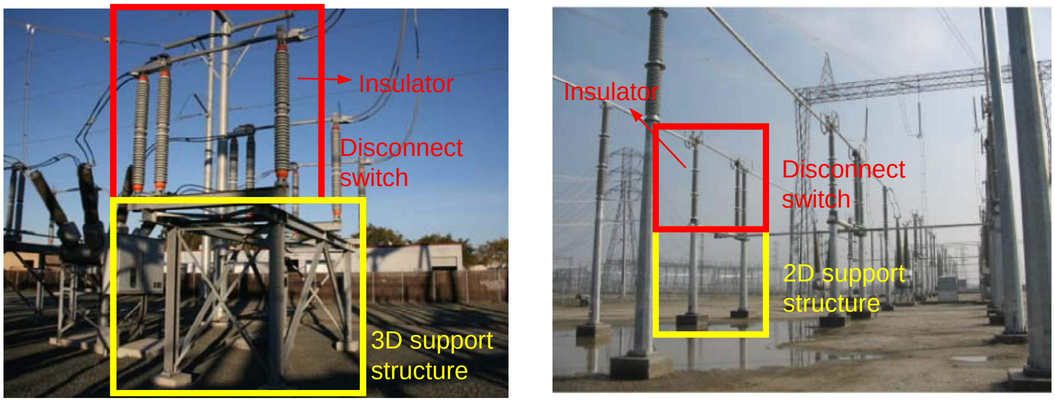

Figure 1.1 Disconnect switches mounted on support structures in field installation.

Figure 1.2 Seismic qualification shaking table tests of 550 kV (left) and 230 kV (right) disconnect switches.

2. BRIEF BACKGROUND ON RTHS ON SMART SHAKING TABLES

A HS test is considered to be conducted in real-time when the experimental substructure is loaded with a rate equal to the computed velocity. Conventional HS with slow rates of loading is sufficient in most cases where rate effects are not important. However, for rate-dependent materials and devices, such as viscous dampers, the recently developed triple friction pendulum bearings or the rate-dependent polymer composite insulators mentioned above, RTHS becomes essential. Dynamic actuators and a digital servo-mechanism have been used by Nakashima et al. (1992) as the first progress of RTHS. After the development of actuator-delay compensation methods by Horiuchi et al. (1999), research on real time HS gained momentum. Although rapid development of computing technologies and control methods increased the number of RTHS research in the recent years (Mercan and Ricles 2007, Bonnet et al. 2008, Bursi et al. 2008 among others), there has been limited applications of real-time HS on a smart shaking table up to date. The use of shaking tables in RTHS similar to the approach used in this paper, where the analytical substructure represents a lower portion of the hybrid structure, has been reported in (Igarashi et al. 2000), (Neild et al. 2005), (Lee et al. 2007), and (Ji et al. 2009). Shao et al. (2011) used a shaking table together with dynamic actuators, where it was possible to model analytical substructures both on top and bottom of the experimental substructure. Recently, Nakata and Stehman (2012) proposed a method that allows the modelling of analytical substructures on the top of the experimental substructure where the experimental substructure is tested on the shaking table without the need to use dynamic actuators. In the coming years, an increase in smart shaking table RTHS applications may be expected, especially with the development of shaking table grids in various laboratories around the world, such as Tongji University or the NEES facilities at the University at Buffalo and the University of California, Berkeley.

3. RTHS FRAMEWORK

Components of the developed RTHS framework, namely the shaking table, controller, data acquisition (DAQ) system and the specimen (insulator), are shown in Fig. 3.1. As marked in the figure, the DAQ system also contains the computational platform through the DSP I/O module. The shaking table employed as a part of the RTHS framework is a small (4 ft × 4 ft [1.22 m x 1.22 m]) high fidelity shaking table at the UC-Berkeley structural testing laboratory, which can reproduce the target accelerations accurately up to 20 Hz frequency (Fig. 3.2). The shaking table is composed of a steel platform moving on supporting rollers. The platform is attached to a 25 kip [111.2 kN], ±5 inch [127 mm] dynamic actuator which can accommodate velocities up to 35 in./sec [889 mm/sec]. Two steel beams placed close to the ends of the platform are used as hold down systems to prevent the uplift due to overturning moments caused by the inertia force of the physical specimen.

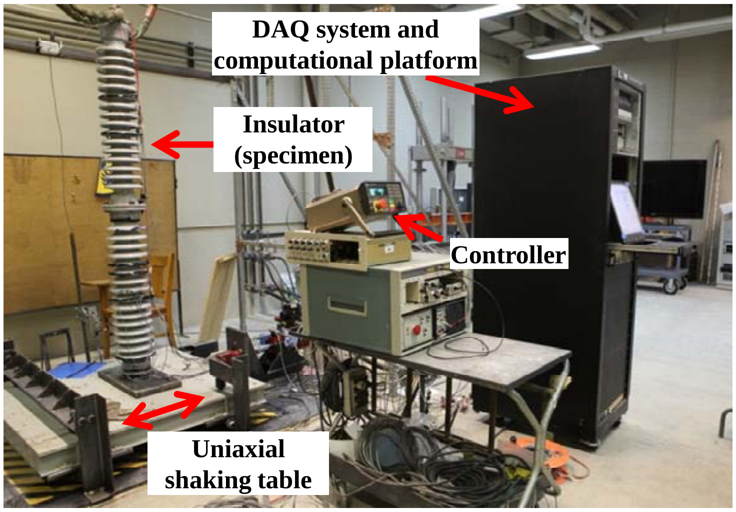

Figure 3.1 Components of the developed RTHS framework.

Figure 3.2 Small (4 ft × 4 ft [1.22 m × 1.22 m]) high fidelity shaking table at UC-Berkeley structural laboratory

Development of the RTHS framework consists of the following four steps: 1) formulation of the governing equation of motion and corresponding computational algorithm, 2) implementation of the computational algorithm in the computational platform, 3) setting up the proper communication between the components of the framework, and 4) adoption of a feed-forward error compensation scheme to minimize the time delay in the actuator response. The key features related to these steps are discussed in the following sub-sections.

3.1 Equation of Motion and Computational Algorithm

In the developed RTHS framework, a single insulator post used in 230 kV disconnect switches is tested as the experimental substructure on a shaking table and a single degree of freedom (SDOF) system representing the support structure is employed as the analytical substructure. It should be noted that testing of a single insulator represents the testing of the disconnect switch in an open configuration where the experimental element is the jaw post as identified by an ellipse in the right-hand side photograph of Fig. 1.2.

According to Fig. 3.3, the governing equation of motion of the mass *m* can be written as follows,

$$m\ddot{u} + c\dot{u} + ku - f = -m\ddot{u}_g \tag{3.1}$$

where *m*, *k* and *c* are respectively the mass, spring stiffness, and damping coefficient of the SDOF analytical substructure that represents the support structure, u, $\dot{u}$ and $\ddot{u}$ are the displacement, velocity and acceleration of the mass with respect to the fixed base of the spring (i.e. base of the support structure), $\ddot{u}_g$ is the ground acceleration time history and *f* is the internal force at the base of the insulator acting on the mass *m*, which is obtained by using load cell measurements during the test. It is worth noting that the force *f* includes the inertial and damping forces acting on the insulator since the HS is conducted in real time.

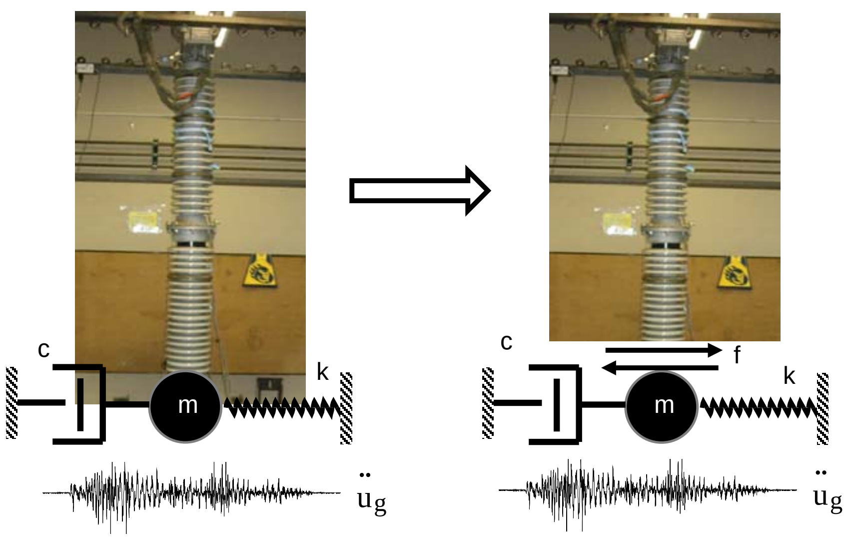

Figure 3.3 Schematic representation of the experimental substructure (insulator jaw post) and SDOF analytical substructure representing the support structure

RTHS is conducted by solving Eqn. 3.1 numerically with explicit Newmark integration (Newmark 1959). Sequence of computations is adjusted to comply with the required HS communications between the experimental and analytical substructures.

3.2 Integration Time Step

With the developed framework, it is possible to conduct RTHS using an integration time step as small as 1 millisecond. Hence, in this case, an integration step is physically completed in 1 millisecond. Such fast execution time of an integration time step is realized by a combination of the computation power introduced by the DSP card, the physical cable transfer between the computational platform and the controller, and the real-time compatible PID control technology of the controller and the servo-hydraulic system. The number of iterations in the used integration scheme of the RTHS should be constant and small in order to be able to allocate a definite and practically applicable time for the completion of each iteration. Moreover, the displacement increments in all the iterations of an integration time step should be as close as possible to each other to avoid velocity and acceleration oscillations within the integration time step. Hence, explicit integration schemes are the most suitable integration methods for RTHS, since they do not require iterations or in other words they require only a single iteration per time step. A limiting factor which restricts the applicability of explicit integration is the conditional stability criterion requiring the integration time step to be smaller than a certain fraction of the period of the highest mode of the structure. In that regard, the ability to use integration time steps as small as 1 millisecond within the developed RTHS framework allows the use of real-time explicit integration compatible to a broad range of analytical and experimental substructure configurations.

Another advantage introduced by the 1 milisecond integration time step is the assurance of continuous movement of the shaking table actuator, since a command is sent to the controller in each millisecond. Accordingly, errors that would be introduced by the application of a predictor-corrector smoothing technique (e.g. Mosqueda 2003) are eliminated.

3.3 Feed-forward Error Compensation

Considerable research has been conducted about the effect of errors on HS. Among the various sources of errors, the problem of phase lag or time delay of the hydraulic actuators is particularly important for RTHS. Phase lag induces not only errors but also negative damping which may lead to instability during RTHS (Nguyen and Dorka, 2009). A simple feed-forward error compensation scheme is implemented in the developed HS framework in order to overcome the time delay problem. This feed-forward error compensation scheme consists of adding the estimated error to the command signal as a function of the actuator velocity. This is a simplified version of the scheme that is proposed by Elkhoraibi and Mosalam (2007). The error function in this study is obtained from the RTHS runs conducted on the bare shaking table. A substantial improvement in the displacement tracking of the shaking table is observed after the implementation of the feed-forward error compensation scheme, Fig. 3.4. It is theoretically possible to achieve a similar error reduction by adjusting the feed-forward gain on the controller. However, this option was not applicable since the feed-forward gain of the utilized controller was limited to 40 miliseconds, which was not sufficient to eliminate the time delay.

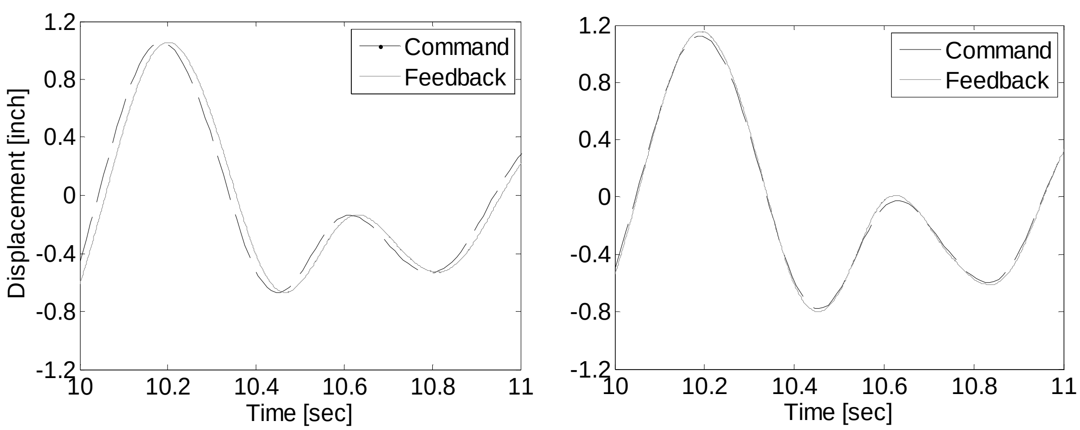

Figure 3.4 Displacement tracking without (left) and with (right) feed-forward error compensation.

4. VERIFICATION OF THE RTHS FRAMEWORK

Proper implementation of the HS algorithm and the measurements used in the algorithm are verified by comparing the RTHS runs conducted for the same set of analytical substructure properties with different scales of the input excitation. The spring in the analytical substructure is defined by a linear force-displacement relationship. In addition, the insulator post, which comprises the experimental substructure, has a linear force-deformation response until failure. Accordingly, the response obtained from one input scale is expected to reproduce that of another scale using the ratio of the applied scales, in the absence of failure of the insulator. The displacement feedback obtained from the position transducer of the actuator is chosen as the response variable for comparison, since this feedback is affected by various components and processes of the RTHS framework; namely the conducted computations including the feed-forward error compensation, the force measurements used in the computations, and the tracking response of the actuator. The displacement feedbacks plotted in Fig. 4.1 verify the above mentioned components and processes of the RTHS framework.

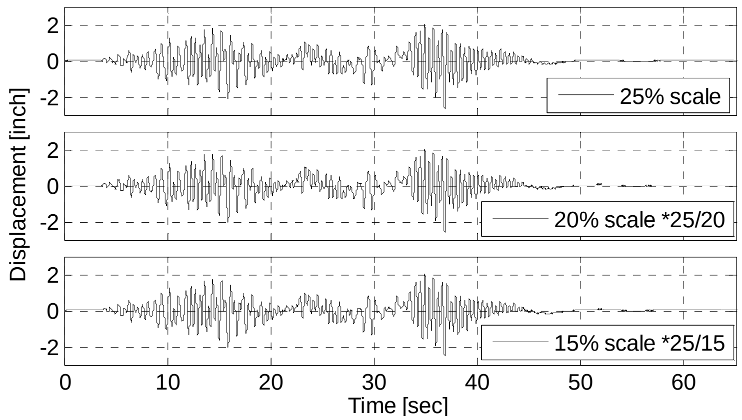

Figure 4.1 Displacement feedback for different input signal scales linearly scaled to 25%.

5. COMPARISON WITH CONVENTIONAL SHAKING TABLE TESTS

The results of a conventional shaking table test are compared with those of the corresponding RTHS test. The conventional shaking table test consists of testing a 230 kV disconnect switch, and its support structure in open configuration (Fig.1.2 right-hand side) on the UC-Berkeley PEER shaking table. In the RTHS, an identical insulator to the one identified with an ellipse is used. As can be noted from Fig. 1.2, the response of the single insulator is independent from the rest of the disconnect switch in the open configuration. Therefore, the response of the marked insulator is compared with the response of the insulator tested with RTHS for validation of the developed RTHS framework. The lateral stiffness and total mass of the support structure tested in the conventional shaking table test is used as the stiffness and mass of the analytical SDOF substructure in RTHS. The employed stiffness (k = 55 kip/in [96.32 kN/cm]) and mass (m = 180 slug [2.63 tonnes]) values are validated by comparing the natural period of the SDOF system with the identified period of the support structure during the shaking table tests. A damping ratio of 1%, identified from the sine sweep tests, is employed in the analytical substructure. The ground motion excitation employed in the tests is an artificially generated excitation from an acceleration record of 1992 Landers earthquake to match the response spectrum required by IEEE693 (IEEE, 2006) at Performance Level (Takhirov et al., 2004).

Acceleration history measured on the top of the support structure and insulator are compared in Fig. 5.1, while the relative displacement of the insulator top with respect to (w.r.t.) the support structure and strain measured at the two sides of the insulator base are plotted in Fig. 5.2 and 5.3, respectively. Accelerations and relative displacements measured in shaking table and RTHS tests are in good agreement. Identical stiffness and mass properties of the insulators tested with the RTHS and shaking table and resemblance of the boundary conditions at the base of the insulators are confirmed from the similar natural frequencies identified for the insulators from both of the tests. Although these frequencies are close to each other (5.13 Hz and 4.87 Hz in RTHS and shaking table test, respectively), the small difference between them maybe the reason for the small differences in the acceleration and displacement responses. The largest deviation between the results of the RTHS and shaking table tests is in the strains although the peak values are very close to each other. Considering that the local response measured by a strain gage can be affected by various conditions including the location and orientation of the gage, local impurities at the cross-section where the strain gage is located, etc., the agreement in the strain gage history shown in Fig. 5.3 and the close match of the peaks can be considered as reasonable.

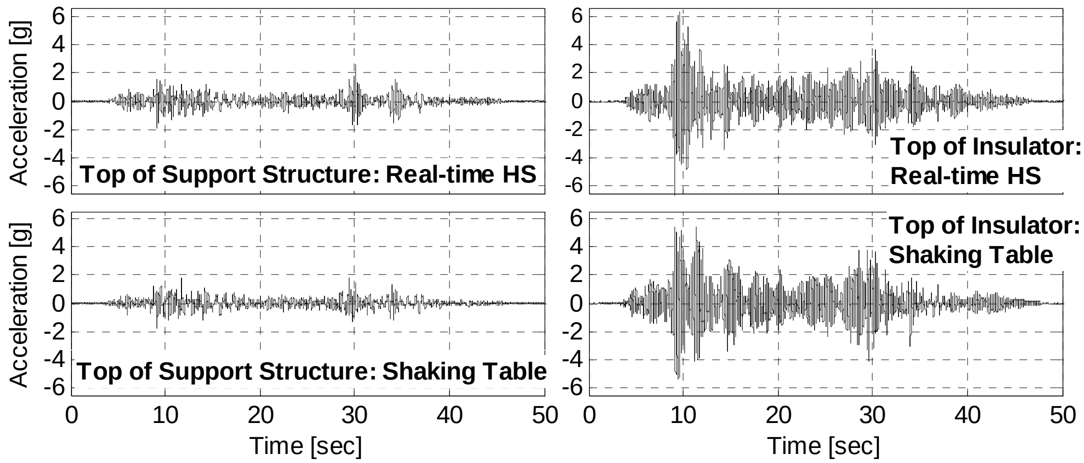

Figure 5.1 Comparison of the accelerations from shaking table and RTHS tests.

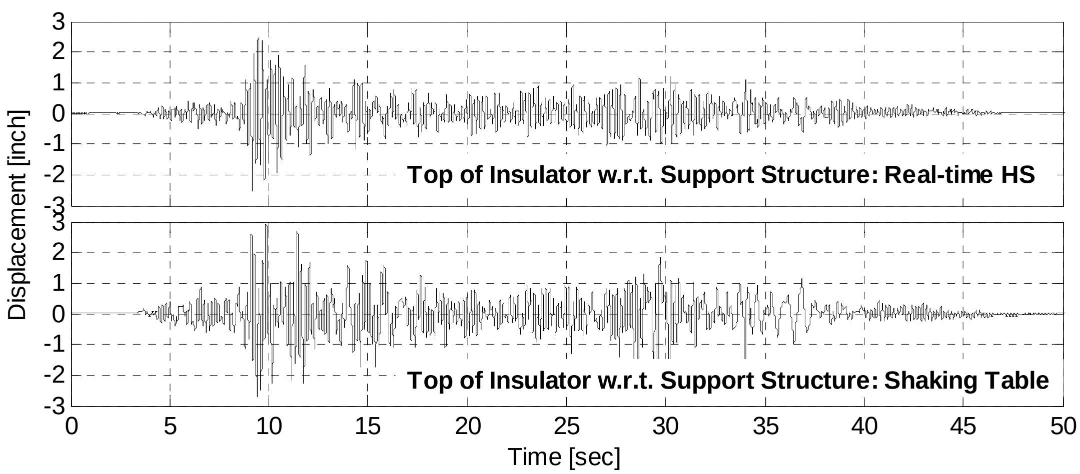

Figure 5.2 Comparison of the relative displacements from shaking table and RTHS tests.

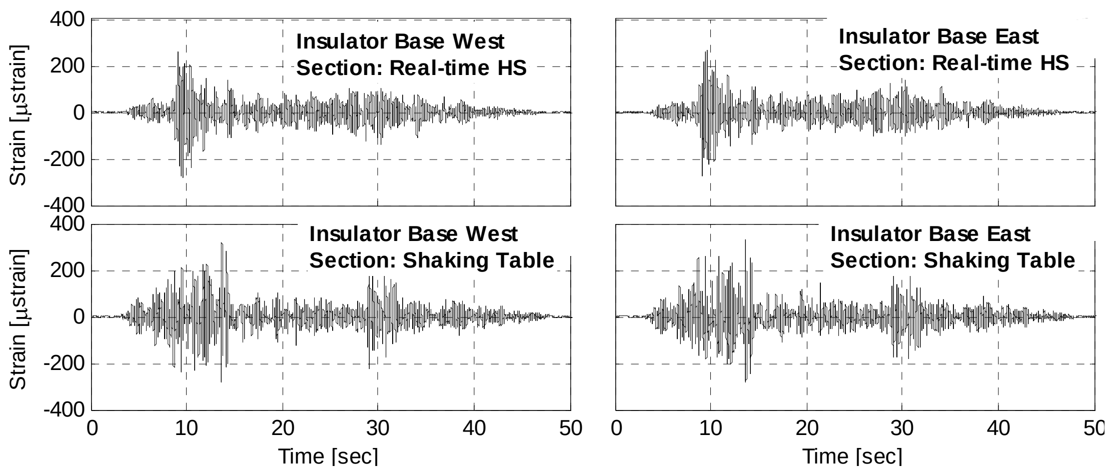

Figure 5.3 Comparison of the strains from shaking table and RTHS tests.

6. EXPERIMENTAL PARAMETRIC STUDY

After validation of the developed RTHS framework, an experimental parametric study is conducted to investigate the effect of support structure stiffness and damping on the insulator response. Among the many conducted tests, the results of 36 tests are reported here. These 36 tests are defined by three damping ratios assigned to the dashpot (*c* in Fig. 3.3 and Eqn. 3.1) of the analytical SDOF system (representing the support structure) and 12 stiffness values assigned to the spring (*k* in Fig. 3.3 and Eqn. 3.1) of the analytical SDOF system, for each damping ratio. Employed damping ratios are 1%, 3%, and 5%, the typical range for steel structures, while the employed stiffness values are provided in Table 6.1. The support structure frequency, f_{ss}, calculated from Eqn. 6.1 with *k* and *m* as shown in Fig. 3.3, and f_{ss} normalized by the insulator frequency, f_{ins} (= 5.13 Hz), are also provided in Table 6.1. It should be noted that f_{ss} and f_{ins} are the uncoupled frequencies of the support structure and insulator, respectively, and the frequencies of the hybrid structure show deviation from these frequencies based on the coupling between the natural modes of the hybrid structure. It is also noted that each of the employed stiffness value corresponds to a different structural configuration of the support structure.

The same ground excitation used in the validation tests is utilized in the parametric study. Parametric study tests are conducted for an input excitation scale of 10%. Such a small scale avoided any source of nonlinearity in the specimen such as grout cracking or loosening of bolts allowing the same unaltered specimen to be tested for all the different analytical spring stiffness and damping values.

Table 6.1 Analytical spring stiffness (*k*) and corresponding frequency values.

k [kip/in]	60.0	55.0	50.0	40.0	35.0	30.0	22.0	16.0	11.0	7.0	4.4	2.2
k [kN/cm]	105.1	96.3	87.6	70.1	61.3	52.5	38.5	28.0	19.3	12.3	7.7	3.9
f_{ss} [Hz]	10.0	9.6	9.2	8.2	7.7	7.1	6.1	5.2	4.3	3.4	2.7	1.9
f_{ss} / f_{ins}	2.0	1.9	1.8	1.6	1.5	1.4	1.2	1.0	0.8	0.7	0.5	0.4

$$f_{ss} = (1/2\pi)\sqrt{k/m} \tag{6.1}$$

Peak strains measured at the insulator base are plotted against f_{ss} (bottom axis) and f_{ss}/f_{ins} (top axis) in Fig. 6.1. Tested porcelain insulators possess a very brittle mode of failure with almost linear elastic response until failure. Therefore, peak strain demand is a very convenient indicator for evaluating the insulator seismic response. Maximum value of peak strain is observed for f_{ss}/f_{ins} close to 1.2 and decreases on either sides of this value. The reason for this number not being equal to 1.0 is the interaction between the experimental and the analytical substructures which in turn leads to the coupling between the modes of the hybrid structure. In other words, in the hypothetical case where the insulator would experience compatible displacement with the support structure without any force transfer (interaction) between the insulator and the support structure, the maximum response would take place at f_{ss}/f_{ins} ratio of 1.0. However, for the real case with force transfer, the maximum peak strain takes place at a different value than unity (i.e. 1.2) for the ratio f_{ss}/f_{ins}. The minimum peak strain occurs for the flexible support structures (f_{ss} < 4 Hz). Hence the flexible support structures seem to be the most suitable for the tested insulator in terms of strain response. It is observed that the effect of the damping ratio of the support structure is highest for f_{ss}/f_{ins} ratios between 0.8 and 1.2 and decreases as this frequency ratio increases or decreases outside this range. In particular, the damping ratio of the support structure has negligible effect for stiff support structures (f_{ss} > 9 Hz). The measured peak strain normalized by the failure strain, determined from static pull-over tests, is also indicated on the right axis of Fig. 6.1. The normalized strain is small because of the 10%-scale of the input excitation.

The porcelain insulators fail in a brittle manner when the tensile stress demand due to bending reaches the capacity. The displacement of an insulator remains in the elastic range as long as no failure is experienced. Hence, the displacements, unlike the strains, are not relevant indicators for the seismic performance evaluation of insulators regarding damage or failure potential. However, the displacements that an insulator experience should be limited in order to prevent pounding effects or damage to the electrical cables and connections. The variations of the peak insulator displacement with frequency and damping of the support structure are shown in Fig. 6.2, where it is observed that the flexible support structures which provide the most suitable strain response do not provide compliant displacement response. Therefore, it is concluded that the stiff support structures (f_{ss} > 9 Hz) constitute the most suitable support structure configuration for the tested insulator concerning both compliant strain and displacement responses. Similar to the case of peak strains, the damping ratio has negligible effect on the insulator displacement for the stiff support structures (f_{ss} > 9 Hz).

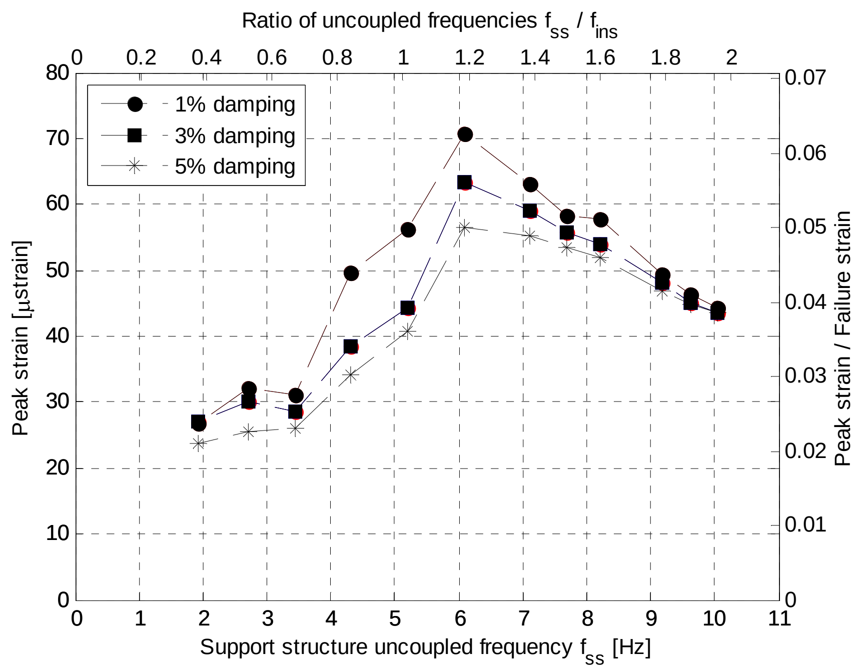

Figure 6.1 Variation of peak strain with damping and frequency of the support structure.

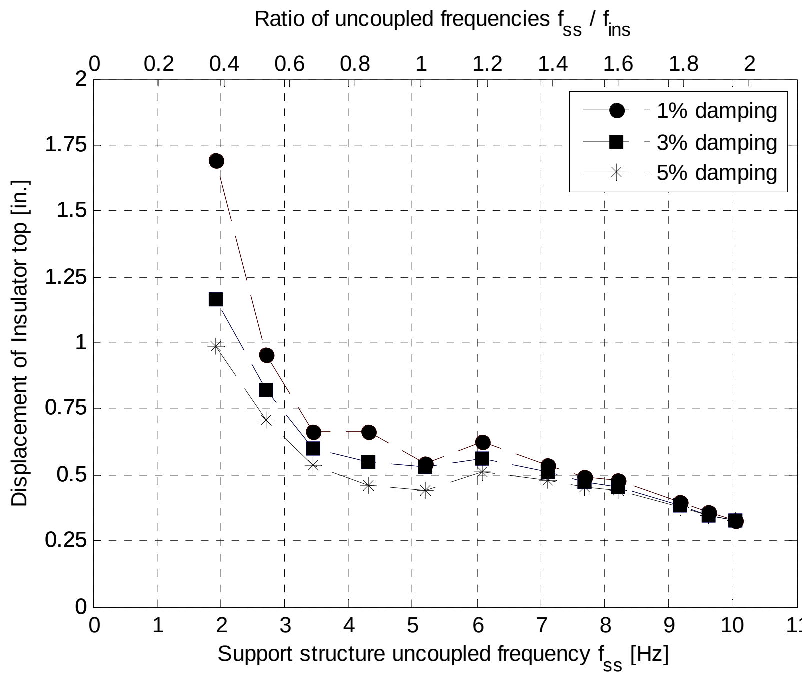

Figure 6.2 Variation of peak displacement with damping and frequency of the support structure.

7. CLOSURE

A RTHS framework is developed for cost effective and timely efficient dynamic testing of electrical insulator posts. Two of the unique features of the developed RTHS framework are the application of a simple feed-forward error compensation scheme and the ability to perform RTHS with integration time steps as small as 1 milisecond. The developed RTHS framework is validated by comparing the RTHS test results with the results of a shaking table test on the whole high voltage electrical switch where close matching of the response measurements, such as accelerations and displacements at the top of the insulator, and local response parameters, such as the strains at the base of the insulator, is observed. After validation of the developed RTHS framework, a parametric study is conducted to investigate the effect of support structure stiffness and damping on the porcelain insulator response. Thirty six different configurations (12 stiffness values and 3 damping ratios) of the support structure are considered in the parametric study and the most suitable support structure configuration is determined for the tested insulator. Such an investigation would require construction and testing of many different support structures, which would probably be practically impossible to realize on a conventional shaking table. Accordingly, the RTHS framework devised in this study can be stated to fulfil the intended objective of cost effective and timely efficient dynamic testing of insulator posts.

AKCNOWLEDGEMENTS

The research was supported by Subcontract TRP-08-02 from California Institute for Energy and Environment. The authors thank M. Moustafa, S. Takhirov and E. Fujisaki for their technical inputs.

REFERENCES

Bonnet, P.A., Williams, M.S. and Blakeborough, A. (2008). Evaluation of numerical time-integration schemes for real time hybrid testing. *Earth. Eng. & Str. Dyn.* **37:13**, 1467-1490.

Bursi, O.S., Gonzalez-Buelga, A., Vulcan, L., Neild, S.A. and Wagg, D.J. (2008). Novel coupling Rosenbrock-based algorithms for real-time dynamic substructure testing. *Earth. Eng. & Str. Dyn.* **37:3**, 339-360.

Elkhoraibi, T. and Mosalam, K.M. (2007). Towards error-free hybrid simulation using mixed variables. *Earth. Eng. & Str. Dyn.* **36:11**, 1497-1522.

Horiuchi, T. and Konno, T. (2001). A new method for compensating delay in time hybrid experiments, *Philosophical Transactions of the Royal Society: Mathematical, Physical & Eng. Sciences* **359**, 1893-1909.

Igarashi, A., Iemura, H. and Suwa, T. (2000). Development of substructured shaking table test method. *12th World Conference on Earthquake Engineering*. Auckland, New Zealand.

IEEE Standard 693-2005. (2006). Recommended Practice for Seismic Design of Substations. New York, NY.

Ji, X., Kajiwara, K., Nagae, T., Enokida, R. and Nakashima, M. (2009). A substructure shaking table test for reproduction of earthquake responses of high-rise buildings. *Earth. Eng. & Str. Dyn.* **38:12**, 1381–1399.

Lee, S., Parka, E., Mina, K. and Park, J. (2007) Real-time substructuring technique for the shaking table test of upper substructures. *Engineering Structures* **29:9**, 2219–2232.

Mercan, O. and Ricles, J.M. (2007). Stability and accuracy analysis of outer loop dynamics in real-time pseudodynamic testing of SDOF systems. *Earth. Eng. and Structural Dynamics* **36:11**, 1523-1543.

Mosqueda, G. (2003). Continuous hybrid simulation with geographically distributed substructures, University of California, Berkeley. *PhD Dissertation*: 232 pages.

Nakashima, M., Kato, M. and Takaoka, E. (1992). Development of real-time pseudo-dynamic testing. *Earth. Eng. & Str. Dyn.* **21:1**, 79-92.

Nakata, N. and Stehman, M. (2012). Substructure shake table test method using a controlled mass: formulation and numerical simulation *Earth. Eng. & Str. Dyn.*, published online 28 Feb.

Neild, S., Stoten, D., Drury, D. and Wagg, D. (2005) Control issues relating to real-time substructuring experiments using a shaking table. *Earth. Eng. & Str. Dyn.* **34:9**, 1171–1192.

Newmark, N.M., (1959). A method of computation for structural dynamics. *ASCE J. Eng. Mec.* **85:EM3**, 67-94.

Nguyen ,N.V. and Dorka, U. (2009). Adaptive error compensation based on online system identification for real-time substructure testing. *Proceedings of the 3rd International Conference on Advances in Experimental Structural Engineering*, October 15-16, San Francisco, CA.

Shao, X., Reinhorn, A.M. and Sivaselvan, M.V. (2011). Real-Time Hybrid Simulation using shake tables and dynamic actuators. *ASCE J. Str. Eng.* **137:7**, 748–760.

Takhirov, S., Fenves, G., Fujisaki, E. and Clyde, D. (2004). Ground motions for earthquake simulator qualification of electrical substation equipment. *PEER Report*. PEER 2004/08.